ARTICLE

Nitrogen-Doped Carbon Nanotubes: High Electrocatalytic Activity toward the Oxidation of Hydrogen Peroxide and Its Application for Biosensing

Xuan Xu,[†] Shujuan Jiang,[‡] Zheng Hu,[‡] and Songqin Liu[†,*]

[†]State Key Laboratory of Bioelectronics, School of Chemistry and Chemical Engineering, Southeast University, Nanjing, 210096, People's Republic of China, and [‡] Key Laboratory of Mesoscopic Chemistry of MOE, School of Chemistry and Chemical Engineering, Nanjing University, Nanjing, 210093, People's Republic of China

ABSTRACT This study compares the electrocatalytic activity of nitrogen-doped carbon nanotubes (NCNTs) with multiwalled carbon nanotubes (MWCNTs). Results indicate that NCNTs possess a marked electrocatalytic activity toward oxygen reduction reaction (ORR) by an efficient four-electron process in the alkaline condition, while the process of MWCNTs is through a two-electron pathway. Meanwhile, NCNTs show a very attractive electrochemical performance for the redox reaction of hydrogen peroxide (H_2O_2) and could be employed as a H_2O_2 sensor at a low potential of +0.3 V. The sensitivity of the NCNT-based biosensor reaches 24.5 μA/mM, more than 87 times that of the MWCNT-based one. Moreover, NCNTs exhibit striking analytical stability and reproducibility, which enables a reliable and sensitive determination of glucose by monitoring H_2O_2 produced by an enzymatic reaction between glucose oxidase/glucose or choline oxidase/choline at +0.3 V without the help of the electron mediator. The NCNT-based glucose biosensor has a linear range from 2 to 140 μM with an extremely high sensitivity of 14.9 μA/mM, and the detection limit is estimated to be 1.2 μM at a signal-to-noise ratio of 3. The results indicate that the NCNTs are good nanostructured materials for potential application in biosensors.

KEYWORDS: nitrogen-doped carbon nanotubes · electrocatalytic · oxygen reduction · hydrogen peroxide · glucose · choline

In the past decade, carbon nanotubes (CNTs) have attracted a great deal of attention in different research fields due to their novel structure, excellent properties, and wide potential applications.[1−7] Most notably, CNT-based sensors possess high sensitivities, low limits of detection, fast electron transfer kinetics, and they have been widely used for the detection of molecules such as NADH,[8] uric acid,[9] homocysteine,[10] ascorbic acid,[11] dopamine,[12] nitric oxide,[13] H_2O_2,[14] glucose,[15] hesperidin,[16] DNA,[17] and TNT.[18] The analytical performances of these sensors depend on the electronic properties, solubility, and biocompatibility of CNTs, which are strongly affected by their surface structures, for example, the number of defective sites and functional groups on the side walls and the ends of CNTs.[19−21] Several strategies, including covalent bonding, physical adsorption, and miscellaneous methods of modification,[22] have been developed for modifying the surfaces of CNTs to impart desired properties such as enhanced sensing capabilities, solubility, and catalytic performance. For example, the defective sites on the CNTs surface could be translated to carboxylic functional groups during the acid treatment process.[19,23] The resultant CNTs possess better dispersion, wettability, and excellent electrocatalytic activity toward the oxidation of homocysteine[10] and ascorbic acid[11] at a low potential. The oxygen-containing groups on the tube surface could redox-mediate the reduction of oxygen in alkaline solution.[24] In addition, some organic compounds with redox-mediation properties, for example, orthoquinone[25] and toluidin blue O[26] are rationally chosen to modify the CNTs through π−π electronic or hydrophobic interactions. The integration of CNTs and a redox mediator leads to sufficient electrocatalysis and paves a new way to functionalization of CNTs for electrochemical applications. Some metal particles can either decorate the walls of the nanotubes[27] or be encapsulated within the interior of the nanotubes to enhance catalytically activity.[28]

On the other hand, doping CNTs with N to yield a large number of defective sites onto the nanotube surfaces is proven to be an efficient method to regulate the structural and electronic properties of the nanotubes.[29−31] For example, different from the case for CNTs, nitrogen-doped CNTs (NCNTs) could be directly used for the immobilization of Pt-based nanoparticles without premodification due to the nitrogen participation, which makes the construction of electrocatalysts much more convenient.[32,33] Dai

*Address correspondence to liusq@seu.edu.cn.

Received for review May 8, 2010 and accepted June 11, 2010.

Published online June 21, 2010. 10.1021/nn1010057

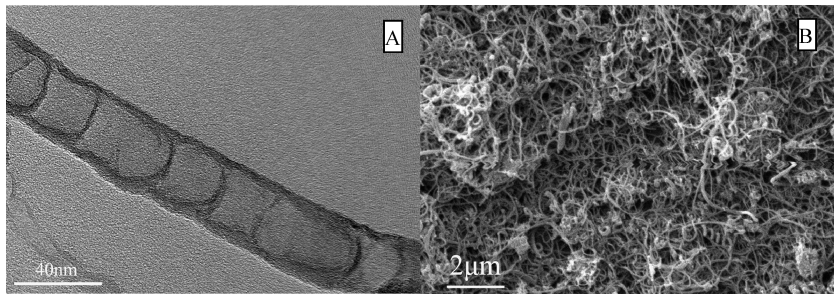

Figure 1. (A) TEM and (B) SEM images of NCNTs.

and his co-workers demonstrated that vertically aligned NCNT (VA-NCNT) itself has high electrocatalytic activity for the oxygen reduction reaction (ORR) in basic electrolyte, indicating its great potential application in fuel cells without using precious metals.[34] Very recently, it was reported that the nitrogen-doped carbon nanotube cups (NCNC) have similar catalytic ability for ORR to that of Pt-CNTs and high electrocatalytic ability toward oxidation of H_2O_2 and glucose.[35] In principle, there is an intrinsic correlation between ORR and redox of H_2O_2, and the electrocatalyst with a low overpotential for ORR should be favorable for H_2O_2 redox.[35] It is noted that ORR overpotential for VA-NCNT (−0.15 V) is much lower than that for NCNC (−0.438 V). This suggests a possibility to greatly improve the performance of the biosensor for the detection of H_2O_2 by exploring suitable NCNTs. In this study, the NCNTs from pyridine precursor were selected for this purpose and the H_2O_2 sensor with excellent sensitivity and stability has been optimized.

RESULTS AND DISCUSSION

The transmission electron microscopy (TEM) image shown in Figure 1A reveals that the as-synthesized NCNTs have a bamboo-shaped structure with a diameter of about 30−35 nm and a "bamboo" segment distance of about 20−40 nm, which may play important roles in their electrocatalytic activities for ORR.[34] After direct casting of the NCNTs suspension onto the electrode surface, the NCNTs are twisted together and a three-dimensional homogeneous incompact membrane can be obtained as shown in the scanning electron microscopy (SEM) image (Figure 1B). The obtained porous membrane of NCNTs possesses good stability and preparation reproducibility. This incompact open structure of NCNT film provides a significant increase of effective active sites for substrates and results in good amperometric response to both oxygen and H_2O_2.

ORR is a rather complex multistep process. In basic solution, ORR involves a four-electron pathway (eq 1), with O_2 reduction directly to water and a two-step, two-electron eq 2 with hydrogen peroxide ion as intermediate product. The main products of ORR are OH^- and HO_2^-, depending on electrode materials, electrode potential, and solution composition.[36]

$$O_2 + 2H_2O + 4e^- \rightarrow 4OH^- \quad (1)$$

$$O_2 + H_2O + 2e^- \rightarrow HO_2^- + OH^- \quad (2)$$

$$HO_2^- + H_2O + 2e^- \rightarrow 3OH^- \quad (3)$$

$$2HO_2^- \rightarrow 2OH^- + O_2 \quad (4)$$

To get better understanding of the ORR route, the linear sweep voltammotric (LSV) measurements were performed for NCNT/GC, MWCNT/GC and bare GC in 0.1 M KOH at a scan rate of 100 mV/s, as shown in Figure 2A. Two reduction peaks located at −0.493/−0.877 and −0.459/−0.975 V were observed for both MWCNT/GC and bare GC, respectively, suggesting the two reduction processes in the potential window employed. The first

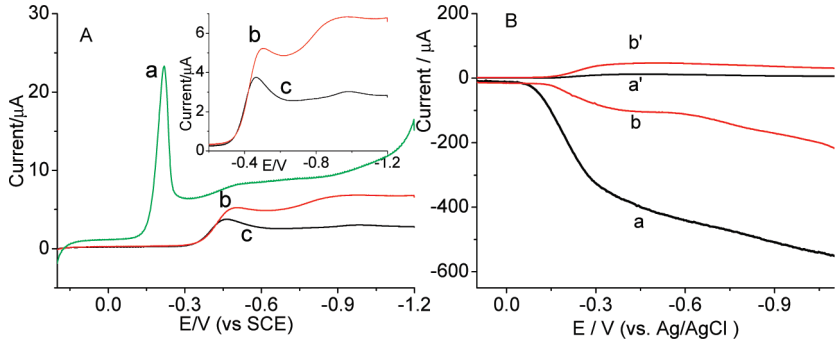

Figure 2. (A) LSV for the ORR at (a) NCNT/GC, (b) MWCNT/GC and (c) bare GC electrodes recorded in an air-saturated 0.1 M KOH solution at room temperature. Scan rate, 100 mV/s. (B) Steady-state voltammograms for NCNTs (curve a and a′) and MWCNTs (curve b and b′) at rotating ring-disk electrode in air saturated 0.1 M KOH electrolyte. The Pt ring electrode was held at 0.5 V while the scan rate was fixed at 10 mV/s. The ring-disk electrode rotation rate was 1400 rpm (rpm).

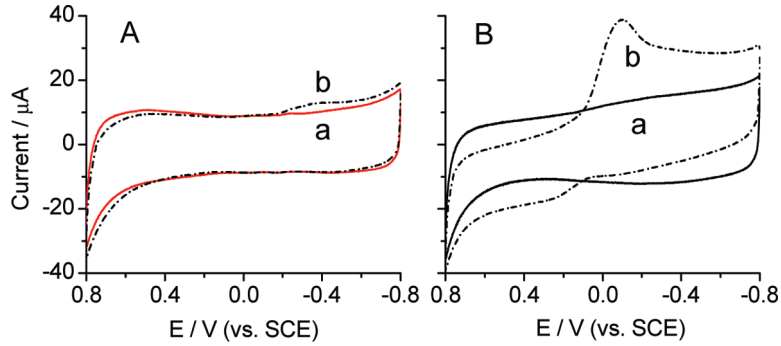

Figure 3. CV curves obtained at (A) MWCNT/GC and (B) NCNT/GC electrodes in 0.10 M, pH 7.4, PBS in the absence (curve a) and presence (curve b) of 17.6 μM H_2O_2 removed oxygen with high purity of N_2 at a scan rate of 50 mV/s.

peaks at −0.493 and −0.459 V were ascribed to the reduction process from O_2 to HO_2^- electrochemically mediated by the oxygen-containing groups (so-called quinine-like group) eq 2, while the second peaks at −0.877 and −0.975 V to a direct 2e reduction pathway eq 3.[24,37] Unlike MWCNT/GC and bare GC, NCNT/GC exhibited only one sharp peak at a rather high potential of −0.218 V. This peak potential is more positive than that of −0.493/−0.877 V at MWCNT/GC and −0.459/−0.975 V at bare GC in this study, and MWCNT-based GC in literatures,[6,24] indicating a different four-electron pathway for ORR in NCNT/GC.

The different ORR routes at CNTs and NCNTs were also evidenced by rotating ring-disk electrode (RRDE) voltammetry under steady-state conditions. Figure 2B showed the steady-state voltammograms for NCNT/GC, MWCNT/GC in air saturated 0.1 M KOH electrolyte. The MWCNT/GC exhibited a two-step process for ORR with the onset potential of about −0.13 and −0.59 V, respectively (curve b). The first step over −0.13 V was attributed to the two-electron reduction of O_2 to HO_2^-, as supported by the increase current corresponding to the oxidation of HO_2^- from −0.1 to −0.43 V at the ring electrode (curve b′).[34,35] However, only one-step process for ORR with the onset potential of about −0.06 V was observed at NCNT/GC (curve a), suggesting a four-electron pathway for ORR at NCNT/GC, which was confirmed by the negligible corresponding current for HO_2^- oxidation recorded at the Pt ring electrode (curve a′). The transferred electron number ($n = 4I_D/(I_D + I_R/N)$, where I_D is the faradic disk current and I_R is the faradic ring current, $N = 0.47$, which is the collection efficiency determined with $Fe(CN)_6^{3-/4-}$ as probe) per oxygen molecule in the ORR process for both MWCNT/GC and NCNT/GC at the potential of −0.40 V was 2.04 and 3.73, respectively.[34,35]

The lower overpotential for NCNT/GC than MWCNT/GC (with shift of 275 mV) suggested that the NCNTs possess a much higher electrocatalytic activity to ORR. Previous study showed that the metal catalyst remaining in the nanotube structure provide activity sites such as FeN_2-C and/or FeN_4-C for enhancement of ORR.[38] After completely removed of the residual Fe catalyst by chemical purification (see XPS in Supporting Information, Figure S1), the observed electrocatalytic activity may be attributed to the nitrogen-induced charge delocalization which changes the chemisorption mode of O_2 from the usual end-on adsorption to a side-on adsorption at the NCNTs surface and effectively weakens the O−O bonding to facilitate ORR.[34] It is noted that the peak potential of our NCNTs (−0.218 V) is much positive to −0.438 V at NCNC modified GC electrode,[35] which suggests the potential application in H_2O_2 detection.

Sensitive detection of H_2O_2 is very important because it is widely applied in many fields such as food, pharmaceutical and environmental analysis.[39,40] H_2O_2 is also product of enzymatic reactions between oxidase and their substrates, thus, substrates can be detected by monitoring the concentration of generated H_2O_2.[41,42] The oxidation of H_2O_2 is the reversed process to ORR where O_2 is reduced to H_2O_2. Due to the high catalytic ability for ORR, the NCNTs were expected to have electrocatalytic activity toward the redox reaction of H_2O_2. Figure 3 showed the typical cyclic voltammograms (CVs) obtained at MWCNT/GC (A) and NCNT/GC (B) in 0.10 M pH 7.4 PBS in the absence (curve a) and presence (curve b) of 17.6 μM H_2O_2. To get rid of the interference of oxygen, the experiments were performed in N_2 saturated solution. A small peak at −0.35 V corresponding to the reduction of H_2O_2 and only slightly increase of the oxidation current at the potential of +0.46 V were observed at MWCNT/GC (Figure 3A). On the other hand, NCNT/GC exhibits a well-defined reduction peak at −0.1 V. The peak potential is 250 mV positive to that at MWCNT/GC, suggesting that NCNT/GC has a higher catalytic activity to the reduction of H_2O_2 than MWCNT/GC. Interestingly, NCNT/GC exhibited an increased oxidation current at the potential of +0.08 V and trended to reach the maximum at +0.25 V. This increase of the oxidation current at NCNT/GC in H_2O_2 containing solution was also observed in LSV measurements with the poten-

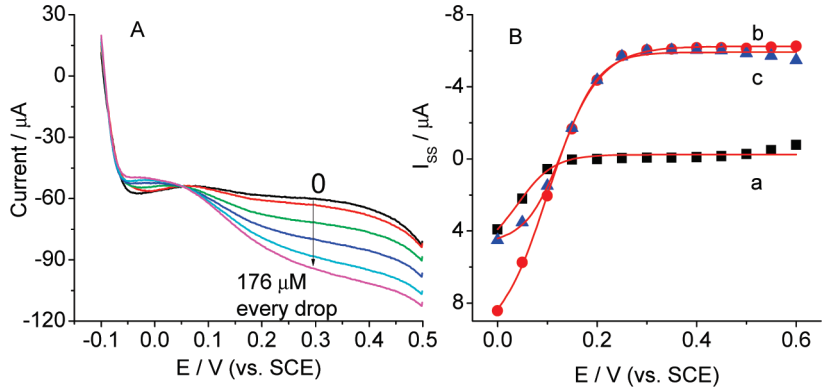

Figure 4. (A) LSVs of NCNT/GC in 0.1 M, pH 7.4 PBS containing 0, 176, 352, 528, 704, and 880 μM H_2O_2 at 100 mV/s. (B) Plots of steady-state current *vs* applied potential at NCNT/GC in 0.1 M pH 7.4 PBS containing (a) 0 and (b) 17.6 μM H_2O_2; (c) is the ratio of the current of (b) to (a).

tial scan from −0.1 to +0.5 V (Figure 4A), suggesting that the increase of the current at +0.25 V could be readily assigned to the oxidation of H_2O_2. In addition, when increasing the H_2O_2 concentration, both the reduction peak current at −0.1 V and oxidation current at +0.25 V increased, which further confirmed that both the reduction and the oxidation responses result from the electrocatalytic reaction of NCNT/GC to H_2O_2. The lower reduction overpotential and increased oxidation current occurred at lower oxidation potential of +0.25 V than those of MWCNTs confirm that NCNTs possess an excellent catalytic activity toward the redox reaction of H_2O_2. This excellent catalytic activity can be used to detect of H_2O_2 concentration at low potential with high sensitivity.

To select the best applied potential for detecting H_2O_2 at NCNT/GC, we performed the control experiment to compare the amperometric response for the same concentration of H_2O_2 at different potentials. The largest amperometric response for the reduction of H_2O_2 was carried out at -0.1 V (data not shown). However, it is hard to remove oxygen completely from the buffer solution and every drop of H_2O_2 into the solution so that the reduction peak current could be attributed to the reduction of both H_2O_2 and oxygen, because NCNTs have high catalytic activity toward ORR as discussed above. Therefore, we choose the oxidation potential for the detection of H_2O_2. With the increase of potential from 0 to +0.6 V, the steady current increases with the increase of the applied potential at NCNT/GC and reaches a constant value at +0.25 V. In consideration of the lower potential and higher sensitivity, we finally selected +0.3 V as the applied potential.

Figure 5 displays a current−time curve of NCNT/GC (a) and MWCNT/GC (b) for successive addition of H_2O_2 in 0.1 M, pH 7.4, PBS at +0.3 V. When H_2O_2 is added into the buffer solution, the oxidation current rises steeply and reaches a stable value. The presence of dissolved oxygen does not affect the response current. Response time of the sensor was less than 2 s. The linear response range of the sensor to H_2O_2 concentration was from 1.76 to 139 μM. The linear regression equation was I_{ss} (μA) = 0.036−0.0245 c (μM), with a correlation coefficient of 0.9999 (inset a in Figure 5). From the slope of 0.0245 μA/μM, the detection limit was estimated to be 0.37 μM at 3σ. The sensitivity of the NCNT/GC to the oxidation of H_2O_2 was 24.5 μA/mM, which was larger than that of 0.28 μA/mM for the MWCNT/GC electrode at +0.3 V (Figure 5b), 13.4 μA/mM at +0.4 V for the TiO_2/MWCNT electrode,[43] 19 nA/mM at −0.3 V for the reduction of H_2O_2 using a carbon nanofiber-modified GC electrode,[44] and 0.19 μA/mM at +0.5 V for NCNC-modified GC electrode.[35]

NCNTs offer a marked decreased overvoltage for the H_2O_2 reaction to allow low-potential amprometric detection. This is of considerable interest to the operation of oxidase-based amperometric biosensors because H_2O_2 will be produced during the en-

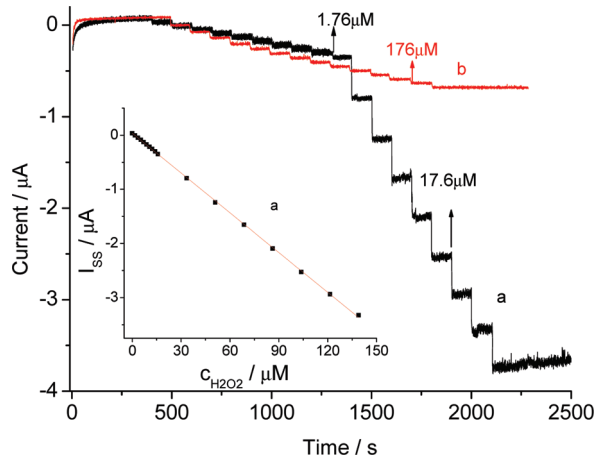

Figure 5. Current−time curve of (a) NCNT/GC and (b) MWCNT/GC electrodes with successive addition of H_2O_2 (indicated by arrows for marked concentrations) in 0.10 M, pH 7.4, PBS at an applied potential of +0.3 V (*vs* SCE). Inset: calibration plots illustrating the linear electrode response to H_2O_2 addition.

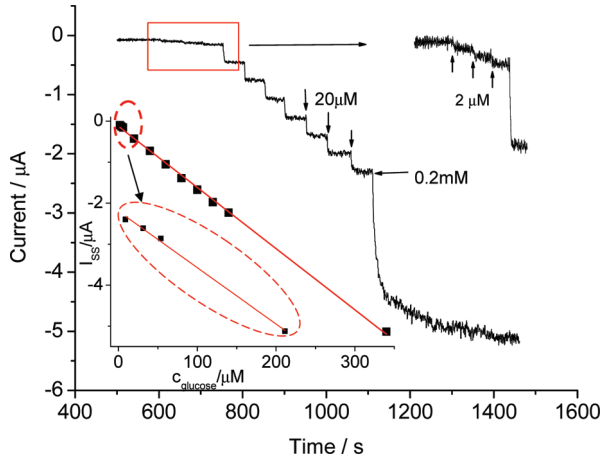

Figure 6. Current−time curve of NCNT/GC electrode with successive addition of glucose to 0.10 M, pH 7.4, PBS solution containing 1 mg/mL GOD at +0.3 V (*vs* SCE). Inset: calibration plots illustrating the linear electrode response to glucose addition.

zyme/glucose reaction. With the assistance of oxygen, the glucose oxidase (GOD) can chemically catalyze the oxidation of glucose to gluconolactone and H_2O_2. As a result, the concentration of glucose can be indirectly detected by determinating of the liberated H_2O_2 in the reaction.

$$\text{glucose} + O_2 \xrightarrow{\text{GOD}} \text{gluconolactone} + H_2O_2$$

$$H_2O_2 \rightarrow 2H^+ + O_2 + 2e^-$$

Figure 6 displayed the amperometric response of the NCNT/GC with successive addition of glucose to 0.1 M, pH 7.4, PBS containing 1 mg/mL GOD at +0.3 V. When glucose is added into the buffer solution, the oxidation current rises steeply to achieve 95% of the steady current in less than 3 s. In contrast, the MWCNT/GC had no response to 20 μM glucose at +0.3 V, which was attributed to its poor behavior in monitoring H_2O_2. Also, no detection signal can be observed at either MWCNT/GC or NCNT/GC in a non-enzyme containing PBS solution. This suggests that the amperometric response of the NCNT/GC upon the addition of glucose to a GOD containing solution is ascribed to the H_2O_2 produced during the enzyme/glucose reaction.

The linear response range of the NCNT/GC to glucose concentration was from 2 to 140 μM. The linear regression equation was I_{ss} (μA) = −0.1227−0.0149 c (μM), with a correlation coefficient of 0.9986 (inset in Figure 6). From the slope of 0.0149 μA/μM, the detection limit was estimated to be 1.2 μM at 3σ. The sensitivity of the NCNT/GC for detection of glucose was 14.9 μA/mM, which was much larger than that of 0.033 μA/mM for NCNC-modified GC electrode[23] with GOD and Nafion at +0.5 V, 0.16 μA/mM for the Pt-CNTs-GOD electrode[45] at −0.1 V and 0.52 μA/mM for the GOD/CNTs/Chitosan/GC electrode[46] at +0.4 V. The stability of NCNT/GC was examined in 0.1 M pH 7.4 PBS containing 1 mg/mL GOD and 20 μM glucose at +0.3 V. The relative standard deviation was 2.9% when successively swept for 100 cycles. The fabrication reproducibility of five electrodes, made independently, showed an acceptable reproducibility with a relative standard deviation of 3.4% for the current determined in 0.1 M pH 7.4 PBS containing 1 mg/mL GOD and 20 μM glucose at +0.3 V.

To further illustrate the universal appeal of this operation of oxidase-based amperometric biosensors, the similar procedure was employed for choline detection, where H_2O_2 will be produced during the follow choline oxidase/choline reaction.

$$\text{choline} + O_2 \xrightarrow{\text{ChOx}} \text{betaine aldehyde} + H_2O_2$$

Figure 7 illustrated the chronoamperometric response of NCNT/GC with successive addition of choline to 0.1 M, pH 7.4, PBS containing 0.5 mg/mL choline oxidase at +0.3 V. Upon a potential step to the sensor in an unstirred system, the reduction current decreases steeply to reach a stable value. With increasing choline concentration, the amperometric response of the NCNT/GC increases. The inset in Figure 7 shows the calibration curve of the NCNT/GC. The linear response range of the NCNT/GC to choline concentration was from 0.1 to 2.9 mM. The linear regression equation was log(−I_{SS}/μA) = 0.9465 + 0.7324 log (c/mM), with a correlation coefficient of 0.9978 (n = 10). From the slope of 0.7324, the detection limit was estimated to be 15 μM at a signal-to-noise ratio of 3. The sensitivity of the NCNT/GC to the oxidation of choline was 5.4 μA/mM.

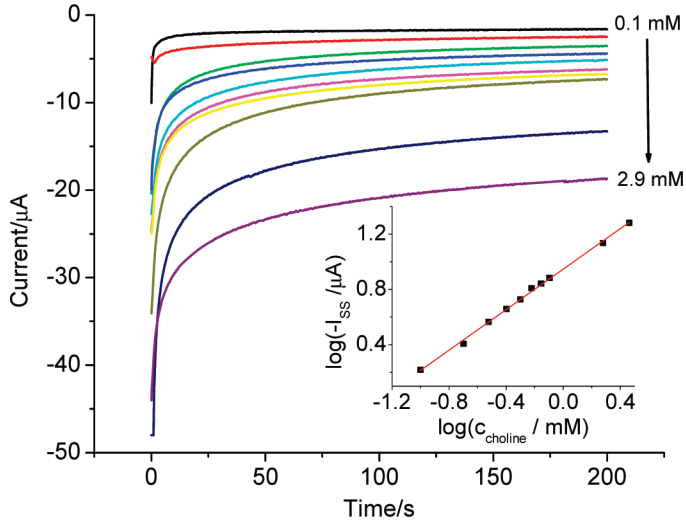

Figure 7. Current−time curve of NCNT/GC electrode with successive addition of 0.1, 0.2, 0.3, 0.4, 0.5, 0.6, 0.7, 0.8, 1.9, and 2.9 mM choline to 0.10 M pH 7.4 PBS solution containing 0.5 mg/mL choline oxidase at +0.3 V (*vs* SCE). Inset: calibration plots illustrating the linear electrode response to choline addition.

CONCLUSION

We have demonstrated that the NCNTs have high electrocatalytic activity toward ORR in alkaline solution and the redox process of H_2O_2. Therefore, the NCNT/GC can be used for monitoring H_2O_2 and glucose/choline at a low potential of +0.3 V with high sensitivity. The results show that the NCNTs are good nanostructured materials with potential application in fuel cells and biosensor construction.

EXPERIMENTAL SECTION

Reagents. NCNTs with a nitrogen content of 3−5% were synthesized by chemical vapor deposition at 650 °C and pyridine was employed as precursor.[47] The as-prepared NCNTs were sequentially refluxed in 6 M NaOH and 6 M HCl aqueous solution at 110 °C for 4 h in turn to remove the Al_2O_3 support and metal catalysts, respectively. The purified NCNTs were thoroughly washed with distilled water until the pH value of the filtrate reached 7 and then dried at 70 °C overnight for further study. CNTs were obtained from Shenzhen Nanotech Port Ltd. Co. (Shenzhen, China), consisting of MWCNTs with a diameter of 10−20 nm and a purity of ~95%. β-D-(+)Glucose and H_2O_2 (30 wt % in water) were purchased from Sinopharm Chemical Reagent Ltd. Co. (Shanghai, China). GOD (EC 1.1.3.4, >100 U/mg), choline oxidase (ChOx, EC 1.1.3.17, from Alcaligenes species, 14.16 units/mg), and choline chloride (purity ≥98%, powder) were obtained from Sigma Aldrich Chem. Co. Other reagents were of analytical reagent grade. Well-dispersed NCNT or CNT suspensions in ethanol with a concentration of 2 mg/mL were prepared under sonication for 30 min. Phosphate buffer solution (PBS; 0.1 M, pH 7.4) was prepared by mixing the stock solution of Na_2HPO_4 and NaH_2PO_4. Distilled water was used throughout the study.

Instrument. Electrochemical measurements were performed on a computer-controlled electrochemical analyzer (CHI832B, CHI Instrument) with the conventional three-electrode system composed of modified glassy carbon electrode (GC) as working electrode, platinum wire as counterelectrode, and saturated calomel electrode (SCE) as reference electrode. A magnetic stirrer provided the convective transport during the amperometric measurement. Rotating ring-disk electrode (RRDE) voltammetry was carried out on a speed controller (HP-1A, Jiangsu, China) and CHI 900C electrochemical workstation (Shanghai, China) using a modified GC ring-disk electrode (5 mm diameter glassy carbon core and 9 mm outer diameter) with a Pt ring polarized at +0.5 V in oxygen atmosphere. The collection efficiency of the rotating ring-disk electrode was determined to be 0.47 with $Fe(CN)_6^{3-/4-}$ as probe. The morphology of the NCNTs modified film was characterized by using scanning electron microscopy (SEM, JEOL JSM-5610LV, Japan) and transmission electron microscopy (TEM, JEOL JEM-100S, Japan).

Electrode Preparation. The GC was successively polished using 1.0 and 0.3 μm alumina powder followed by rinsing thoroughly with doubly distilled water. After successive sonication in 1:1 nitric acid, acetone, and doubly distilled water, the electrode was rinsed with doubly distilled water and dried at room temperature. A 10 μL 2 mg/mL of NCNT or MWCNT suspension was dropped on the surface of the pretreated GC (or 5 μL 2 mg/mL of NCNT or MWCNT suspension was dropped on the GC disk part for RRDE) and dried under vacuum to obtain NCNT-modified GC electrode (NCNT/GC) and MWCNT-modified GC electrode (MWCNT/GC). Electrolyte was a 0.1 M KOH solution for ORR, 0.1 M pH 7.4 PBS for reduction of H_2O_2, and 0.1 M pH 7.4 PBS containing 1 mg/mL GOD or 0.5 mg/mL ChOx for glucose or choline detection, respectively.

Acknowledgment. The project is supported by the National Basic Research Program of China (No. 2010CB732400), National Natural Science Foundation of China (Grant Nos. 20675013 and 20875013), Technology Support Programme of Jiangsu Province (SBE200900289), and the Specialized Research Funds for the Doctoral Program of Higher Education (200802860035).

Supporting Information Available: X-ray photoelectron spectroscopic (XPS, Kratos AXIS UltraDLD Ultrahigh Vacuum (UHV) surface analysis system, Kratos Analytical Ltd., U.K.) is used to characterize the NCNTs after chemical purification. This material is available free of charge *via* the Internet at http://pubs.acs.org.

REFERENCES AND NOTES

1. Iijima, S. Helical Microtubules of Graphitic Carbon. *Nature* **1991**, *354*, 56–58.
2. Rao, C. N. R.; Satishikumar, B. C.; Govindaraj, A.; Nath, M. Nanotubes. *ChemPhysChem* **2001**, *2*, 78–105.
3. Haughman, R. H.; Zakhidov, A. A.; de Heer, W. A. Carbon Nanotubes: The Route Toward Applications. *Science* **2002**, *297*, 787–792.
4. Ajayan, P. M. Nanotubes from Carbon. *Chem. Rev.* **1999**, *99*, 1787–1799.
5. Ju, S. Y.; Kopcha, W. P.; Papadimitrakopoulos, F. Brightly Fluorescent Single-Walled Carbon Nanotubes *via* an Oxygen-Excluding Surfactant Organization. *Science* **2009**, *323*, 1319–1323.
6. Heller, D. A.; Baik, S.; Eurell, T. E.; Strano, M. S. Single-Walled Carbon Nanotube Spectroscopy in Live Cells: Towards Long-Term Labels and Optical Sensors. *Adv. Mater.* **2005**, *17*, 2793–2799.
7. Chen, J.; Perebeinos, V.; Freitag, M.; Tsang, J.; Fu, Q.; Liu, J.; Avouris, P. Bright Infrared Emission from Electrically Induced Excitons in Carbon Nanotubes. *Science* **2005**, *310*, 1171–1174.
8. Mustafa, M.; Wang, J.; Merkoci, A.; Lin, Y. Low-Potential Stable NADH Detection at Carbon-Nanotube-Modified Glassy Carbon Electrodes. *Electrochem. Commun.* **2002**, *4*, 743–746.
9. Rodriguez, M. C.; Sandoval, J.; Galicia, L.; Gutierrez, S.; Rivas, G. A. Highly Selective Determination of Uric Acid in the Presence of Ascorbic Acid at Glassy Carbon Electrodes Modified with Carbon Nanotubes Dispersed in Polylysine. *Sens. Actuators, B* **2008**, *134*, 559–565.
10. Gong, K. P.; Dong, Y.; Xiong, S. X.; Chen, Y.; Mao, L. Q. Novel Electrochemical Method for Sensitive Determination of Homocysteine with Carbon Nanotube-Based Electrodes. *Biosens. Bioelectron.* **2004**, *20*, 253–259.
11. Zhang, M. N.; Liu, K.; Xiang, L.; Lin, Y. Q.; Su, L.; Mao, L. Q. Carbon Nanotube-Modified Carbon Fiber Microelectrodes for *In Vivo* Voltammetric Measurement of Ascorbic Acid in Rat Brain. *Anal. Chem.* **2007**, *79*, 6559–6565.
12. Phillips, P. E.; Stuber, G. D.; Heien, M. L.; Wightman, R. M.; Carelli, R. M. Subsecond Dopamine Release Promotes Cocaine Seeking. *Nature* **2003**, *422*, 614–618.
13. Wu, F. H.; Zhao, G. C.; Wei, X. W. Electrocatalytic Oxidation of Nitric Oxide at Multi-Walled Carbon Nanotubes Modified Electrode. *Electrochem. Commun.* **2002**, *4*, 690–694.
14. Wang, J.; Musameh, M.; Lin, Y. Solubilization of Carbon Nanotubes by Nafion toward the Preparation of Amperometric Biosensors. *J. Am. Chem. Soc.* **2003**, *125*, 2408–2409.
15. Meng, L.; Jin, J; Yang, G. X.; Lu, T. H.; Zhang, H.; Cai, C. X. Nonenzymatic Electrochemical Detection of Glucose Based on Palladium-Single-Walled Carbon Nanotube Hybrid Nanostructures. *Anal. Chem.* **2009**, *81*, 7271–7280.
16. Sims, M. J.; Wildgoose, G. G.; Compton, R. G. Using Multiwalled Carbon Nanotube Modified Electrodes for the Adsorptive Striping Voltammetric Determination of Hesperidin. *Electrochim. Acta* **2009**, *54*, 5030–5034.
17. Napier, M. E.; Hull, D. O.; Thorp, H. H. Electrocatalytic Oxidation of DNA-Wrapped Carbon Nanotubes. *J. Am. Chem. Soc.* **2005**, *127*, 11952–11953.
18. Wang, J.; Hocevar, S. B.; Ogorevc, B. Carbon Nanotube-Modified Glassy Carbon Electrode for Adsorptive Stripping

Voltammetric Detection of Ultratrace Levels of 2,4,6-Trinitrotoluene. *Electrochem. Commun.* **2004**, *6*, 176–179.
19. Banks, C. E.; Moore, R. R.; Davis, T. J.; Compoton, R. G. Investigation of Modified Basal Plane Pyrolytic Graphite Electrodes: Definitive Evidence for the Electrocatalytic Properties of the Ends of Carbon Nanotubes. *Chem. Commun.* **2004**, *16*, 1804–1805.
20. Lin, Y.; Taylor, S.; Li, H. P.; Fernando, K. A. S.; Qu, L. W.; Wang, W.; Gu, L. R.; Zhou, B.; Sun, Y. P. Advances toward Bioapplication of Carbon Nanotubes. *J. Mater. Chem.* **2004**, *14*, 527–541.
21. Davis, J. J.; Green, M. H. L. H.; Hill, H. A. O.; Leung, Y. C.; Sadler, P. J.; Sloan, J.; Xavier, A. V.; Tsang, S. C. The Immobilisation of Proteins in Carbon Nanotubes. *Inorg. Chim. Acta* **1998**, *272*, 261–266.
22. Gregory, G.; Wildgoos, G. G.; Banks, C. E.; Leventis, H. C.; Compton, R. G. Chemically Modified Carbon Nanotubes for Use in Electroanalysis. *Microchim. Acta* **2006**, *152*, 187–214.
23. Banks, C. E.; Davies, T. J.; Wildgoose, G. G.; Compoton, R. G. Electrocatalysis at Graphite and Carbon Nanotube Modified Electrods: Edge-Plane Sites and Tube Ends Are the Reactive Sites. *Chem. Commun.* **2005**, *7*, 829–841.
24. Zhang, M. N.; Yan, Y. M.; Gong, K. P.; Mao, L. Q.; Guo, Z. X.; Chen, Y. Electrostatic Layer-by-Layer Assembled Carbon Nanotube Multilayer Film and Its Electrocatalytic Activity for O_2 Reduction. *Langmuir* **2004**, *20*, 8781–8785.
25. Gong, K. P.; Zhu, X. Z.; Zhao, R.; Xiong, S. X.; Mao, L. Q.; Chen, C. F. Rational Attachment of Synthetic Triptycene Orthoquinone onto Carbon Nanotubes for Electrocatalysis and Sensitive Detection of Thiols. *Anal. Chem.* **2005**, *77*, 8158–8165.
26. Zhang, M. G.; Gorski, W. Electrochemical Sensing Platform Based on the Carbon Nanotubes/Redox Mediators-Biopolymer System. *J. Am. Chem. Soc.* **2005**, *127*, 2058–2059.
27. Kumar, M. K.; Ramaprabhu, S. Nanostructured Pt Functionlized Multiwalled Carbon Nanotube Based Hydrogen Sensor. *J. Phys. Chem. B* **2006**, *110*, 11291–11298.
28. Sloan, J.; Hammer, J. The Opening and Filling of Single Walled Carbon Nanotubes (SWTs). *Chem. Commun.* **1998**, *3*, 347–348.
29. Yang, Q. H.; Hou, P. X.; Unno, M.; Yamauchi, S.; Saito, R.; Kyotani, T. Dual Raman Features of Double Coaxial Carbon Nanotubes with N-Doped and B-Doped Multiwalls. *Nano Lett.* **2005**, *5*, 2465–2469.
30. Katz, E.; Willner, I. Biomolecule-Functionalized Carbon Nanotubes: Applications in Nanobioelectronics. *ChemPhysChem* **2004**, *5*, 1084–1104.
31. Jang, J. W.; Lee, C. E.; Lyu, S. C.; Lee, T. J.; Lee, C. Structual Study of Nitrogen-Doped Effects in Bamboo-Shaped Multiwalled Carbon Nantubes. *Appl. Phys. Lett.* **2004**, *84*, 2877–2879.
32. Yue, B.; Ma, Y. W.; Tao, H. S.; Yu, L. S.; Jian, G. Q.; Wang, X. Z.; Wang, X. S.; Lu, Y. N.; Hu, Z. CNx Nanotubes as Catalyst Support to Immobilize Platinum Nanoparticles for Methanol Oxidation. *J. Mater. Chem.* **2008**, *18*, 1747–1750.
33. Jiang, S. J.; Ma, Y. W.; Jian, G. Q.; Tao, H. S.; Wang, X. Z.; Fan, Y. N.; Lu, Y. N.; Hu, Z.; Chen, Y. Facile Construction of Pt-Co/CNx Nanotube Electrocatalysts and Their Application to the Oxygen Reduction Reaction. *Adv. Mater.* **2009**, *21*, 4953–4956.
34. Gong, K. P.; Du, F.; Xia, Z. H.; Durstock, M.; Dai, L. M. Nitrogen-Doped Carbon Nanotube Arrays with High Electrocatalytic Activity for Oxygen Reduction. *Science* **2009**, *323*, 760–764.
35. Tang, Y. F.; Allen, B. L.; Kauffman, D. R.; Star, A. Electrocatalytic Activity of Nitrogen-Doped Carbon Nanotube Cups. *J. Am. Chem. Soc.* **2009**, *131*, 13200–13201.
36. Shen, Y.; Wittstock, G. Detection of Hydrogen Peroxide Produce during Electrochemical Oxygen Reduction Using Scanning Electrochemical Microscopy. *Anal. Chem.* **2008**, *80*, 750–759.
37. Gong, K. P.; Yu, P.; Su, L.; Xiong, S. X.; Mao, L. Q. Polymer-Assisted Synthesis of Manganese Dioxide/Carbon Nanotube Nanocomposite with Excellent Electrocatalytic Activity toward Reduction of Oxygen. *J. Phys. Chem. C* **2007**, *111*, 1882–1887.
38. Yang, J.; Liu, D. J.; Kariuki, N. N.; Chen, L. X. Aligned Carbon Nanotues with Built-in FeN_4 Active Sites for Electrocatalytic Reduction of Oxygen. *Chem. Commun.* **2008**, *3*, 329–331.
39. Wang, J.; Lin, Y.; Chen, L. Organic-Phase Biosensors for Monitoring Phenol and Hydrogen-Peroxide in Pharmaceutical Antibacterial Products. *Analyst* **1993**, *118*, 277–280.
40. Forzani, E. S.; Rivas, G. A.; Solis, V. M. Amperometric Determination of Dopamine on an Enzymatically Modified Carbon Paste Electrode. *J. Electroanal. Chem.* **1995**, *382*, 33–40.
41. Hrapovic, S.; Liu, Y.; Male, K. B.; Luong, J. H. T. Electrochemical Biosensing Platforms Using Platinum Nanoparticles and Carbon Nanotubes. *Anal. Chem.* **2004**, *76*, 1083–1088.
42. Wang, J. Electrochemical Glucose Biosensors. *Chem. Rev.* **2008**, *108*, 814–825.
43. Jiang, L. C.; Zhang, W. D. Electrodeposition of TiO_2 Nanoparticles on Multiwalled Carbon Nanotube Arrays for Hydrogen Peroxide Sensing. *Electroanalysis* **2009**, *21*, 988–993.
44. Wu, L. N.; Zhang, X. J.; Ju, H. X. Highly Sensitive Flow Injection Detection of Hydrogen Peroxide with High throughput Using a Carbon Nanofiber-Modified Electrode. *Analyst* **2007**, *132*, 406–408.
45. Wen, Z. H.; Ci, S. Q.; Li, J. H. Pt Nanoparticles Inserting in Carbon Nanotube Arrays: Nanocomposites for Glucose Biosensors. *J. Phys. Chem. C* **2009**, *113*, 13482–13487.
46. Liu, Y.; Wang, M. K.; Zhao, F.; Xu, Z. A.; Dong, S. J. The Direct Electron Transfer of Glucose Oxidase and Glucose Biosensor Based on Carbon Nanotubes/Chitosan Matrix. *Biosens. Bioelectron.* **2005**, *21*, 984–988.
47. Chen, H.; Yang, Y.; Hu, Z.; Huo, K. F.; Ma, Y. W.; Chen, Y.; Wang, X. S.; Lu, Y. N. Synergism of C_5N Six-Membered Ring and Vapor-Liquid-Solid Growth of CNx Nanotubes with Pyridine Precursor. *J. Phys. Chem. B* **2006**, *110*, 16422–16427.